Gold Nanospheres as Inhibitors of Amyloid-β Protein Aggregation Involved in Alzheimer's Disease

Mihyun Lim[1], Deborah Soto-Ortega[2], Rahina Mahtab[3] and Melissa A. Moss[4]

[1]*Department of Biological Sciences, University of South Carolina*
[2]*Biomedical Engineering Program, University of South Carolina*
[3]*Department of Biology and Physical Sciences, South Carolina State University*
[4]*Department of Chemical Engineering, University of South Carolina*

Received October, 2011

Alzheimer's disease (AD) is hypothesized to be caused by the amyloid-β protein (Aβ), which aggregates into β-sheet structure to form thick, twisted fibrils that deposit in the brain as insoluble plaques. Thus, finding inhibitors that prevent or reduce the aggregation of Aβ would be one therapeutic strategy for fighting this disease. Gold nanoparticles are ideal candidates for this therapeutic strategy for AD. Nanoparticles are small enough for human cells to uptake but won't induce cell death. Nanoparticles can also cross the blood-brain barrier (BBB) at low concentrations. Thus, we investigated the inhibitory capabilities of gold nanoparticles by performing monomer aggregation assays using gold nanospheres with three different coatings: citrate, poly (acrylic acid) (PAA), and poly (allylamine hydrochloride) (PAH). Aβ monomer was incubated in the presence or absence of nanospheres and agitated to promote aggregation. β-sheet aggregates formed were monitored using thioflavin T (ThT), a fluorescent dye that binds the β-sheet structure of amyloid aggregates but not random coil monomer to yield an enhanced signal. Results demonstrate that gold nanospheres do inhibit Aβ aggregate formation, and this inhibition is influenced by both surface coating and nanoparticle size. 18 nm PAA coated nanospheres were identified as potent inhibitors, capable of abrogating aggregation at a substoichiometric ratio of 1:200.

Introduction

Alzheimer's disease (AD) is a progressive neurodegenerative disorder that results in memory loss, unusual behavior, inabilities to think or process, and, eventually, death [1]. AD patients also exhibit behavioral problems, such as agitation, irritability, and aggression, which make it more difficult for the caregivers to deal with the patients. AD patients eventually lose themselves in confusion, are unable to recognize their loved ones, and gradually become unable to carry on their basic daily function, thus requiring 24/7 standby-assistants, contributing emotional and economic burden to their families. Because the risk of AD exacerbates with age, and since the life expectancy is increasing, this brings an even bigger challenge to health care. Currently, it is estimated that there are 25-30 million AD patients worldwide, and studies suggest that the number of AD cases will triple by 2040 [2]. With the growing population and an increasing life expectancy, a therapeutic strategy for AD is even more dire than ever.

This devastating disease was first discovered by and named after Dr. Alois Alzheimer. In 1901, he admitted a 51-year old patient, named Auguste D. with progressive memory loss, hallucination, and delusion. Intrigued by such odd behaviors, Dr. Alzheimer investigated her brain post-mortem and found unusual deposits in the brain tissues that he identified as neuritic plaques [3]. These plaques were later found to be comprised of the amyloid-β protein (Aβ). Soluble Aβ monomer aggregates to form insoluble Aβ fibrils that deposit in the brain as plaques. These cytotoxic plaques could trigger microglial activation followed by neuritic degeneration [2]. Such degeneration leads to neuronal loss, causing the brains of AD patients to weigh one-third less than that of normal aging subjects [4]. Another study suggests that accumulation of Aβ deposits at synaptic terminals may cause synaptic damage related to cognitive decline [5]. Therefore, finding inhibitors that prevent or reduce the aggregation of Aβ is one therapeutic strategy for fighting this disease.

Nanoparticles have been explored for their utility in a number of medical applications. Nanoparticles have been used for cell imaging, targeted drug delivery, cancer diagnostics and therapeutic applications [6]. In applications of AD treatment, nanoparticles are attractive candidates as a result of their demonstrated ability to penetrate the blood brain barrier (BBB) [7]. In fact, nanoparticles have been shown to affect Aβ aggregation. Yoo et al. demonstrate a promotion of Aβ aggregation by *N*-isopropylacrylamide and *N-tert*-butylacrylamide copolymeric nanoparticles as well as cerium oxide nanoparticles. These researchers hypothesize that electrostatic interactions between nanoparticles and proteins lead to an increased local protein concentration in the vicinity of the nanoparticles, which accelerates the nucleation-dependent aggregation process. In contrast, cadmium telluride (CdTe) nanoparticles have been shown to slow the rate of Aβ aggregation by binding protein to deplete the

amount of free monomers available for aggregate formation [8].

In addition, Cabaleiro-Logo et al. report that copolymeric nanoparticles of varying hydrophobicity not only prevent aggregation by binding to monomeric Aβ and prefibrillar oligomers but also reverse the aggregation of Aβ fibrils formed in absence of these nanoparticles [9].

In the current study, we explore the ability of spherical gold nanoparticles (AuNPs) to attenuate Aβ aggregation. Spherical AuNPs are an ideal candidate as an AD therapeutic because they are small enough for human cells to uptake (10) and are not cytotoxic (10, 11). In addition, AuNP can be easily characterized using UV-Vis spectrophotometry and transmission electron microscopy (TEM) [6].

We investigated the inhibitory capabilities of AuNPs with three different surface coatings: citrate, poly (acrylic acid) (PAA), and poly (allylamine hydrochloride) (PAH). We demonstrate that both surface coating and nanoparticle size can influence inhibitory capabilities. Furthermore, we identify 18 nm PAA coated AuNPs as strong inhibitors of Aβ aggregation that are capable of abrogating aggregate formation at a substoichiometric ratio of 1:200.

Materials and Methods

Materials

$A\beta_{1\text{-}40}$ peptide, thioflavin T (ThT), and bovine serum albumin (BSA) were purchased from Anaspec, Inc. (San Jose, CA), Sigma (St. Louis, MO), and EMD Biosciences (San Diego, CA), respectively.

$A\beta_{1\text{–}40}$ Monomer Purification

$A\beta_{1\text{-}40}$ monomer was purified to remove small aggregates that could serve as nucleation seeds. $A\beta_{1\text{-}40}$ protein was stored desiccated at -20°C. The protein was solubilized to a concentration of 2 mg/mL in 50 mM NaOH and purified via size exclusion chromatography (SEC) on a Superdex 75 HR10/300 column (GE Healthcare, Buckinghamshire, UK). Prior to $A\beta_{1\text{-}40}$ monomer purification, the column was equilibrated in 40 mM Tris-HCl, pH 8.0, and pretreated with 2 mg/mL BSA to reduce any nonspecific interaction between the column matrix and the peptide. UV-Vis absorbance (276 nm) was used to calculate the purified $A\beta_{1\text{-}40}$ monomer concentration using an extinction coefficient of 1450 $M^{-1} \cdot cm^{-1}$.

$A\beta_{1\text{–}40}$ Monomer Aggregation

SEC-purified $A\beta_{1\text{-}40}$ monomer at a concentration of 40 μM was incubated alone (control) or with 0.02 nM, 0.1 nM, or 0.2 nM gold nanoparticles in 40 mM Tris-HCl, pH 8.0. These solutions were agitated via vortexing at 800 rpm and 25°C to promote aggregation. β-sheet aggregate formation was monitored using ThT, a fluorescent dye that binds the β-sheet structure of amyloid aggregates but not random coil monomer to yield an enhanced signal. Periodically, an aliquot was diluted eightfold into 10 μM ThT and the fluorescence was measured using an LS-45 luminescence spectrometer (Perkin–Elmer,Waltham, MA) with excitation at 450 nm and emission from 470 nm to 500 nm. Fluorescence values were determined as the area under the emission peak.

Aβ monomer aggregation exhibits three distinct phases: lag, growth, and plateau. During the lag phase, nucleation occurs, followed by a growth phase during which the amount of β-sheet aggregate increases rapidly. Eventually, the aggregation process reaches a plateau, where monomers and aggregates of different sizes are in equilibrium. An effective inhibitor will reduce the height of the plateau. Reduction of the equilibrium plateau for aggregate formation, PR, is calculated as Eq. 1:

$$PR = \left(1 - \frac{F_I}{F_C}\right) \times 100\% \quad (1)$$

where F_I is the fluorescence of the plateau observed in the presence of the inhibitor and F_C is the fluoresce of the plateau observed for the control.

Gold Nanoparticles

8 nm and 18 nm gold nanoparticles (AuNP) were a kind gift from the laboratory of Dr. Rahina Mahtab at South Carolina State University. As shown in Figure 1, AuNPs with four different coatings were tested for their inhibitory capabilities. AuNPs were created by a series of surface overcoatings. First, following the Frens method, the reduction of hydrogen tetrachloroaurate (III) trihydrate ($HAuCl_4$) by sodium citrate created negatively charged citrate coated AuNPs. For poly (acrylic acid) (PAA) AuNPs, 3 nm citrate AuNPs were synthesized via the reduction of $HAuCl_4$ by sodium borohydride and then capped with sodium citrate. Using ascorbic acid, a solution of $HAuCl_4$ and hexadecyltrimethylammonium bromide (CTAB) was weakly reduced and then added to the 3 nm seeds to increase their diameter, growing from 8 nm to 18 nm (12). Once the CTAB particles were created to the desired size, PAA was overcoated onto the particles to yield negatively charged PAA AuNPs. PAA AuNPs were overcoated to yield positively charged poly (allylamine hydrochloride) (PAH) AuNPs.

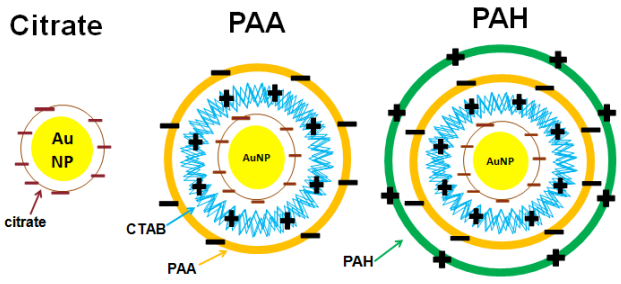

Figure 1. Citrate AuNPs overcoated with CTAB, PAA, and PAH to yield AuNPs with different surface properties.

Results and Discussion

When $A\beta_{1\text{-}40}$ monomer was aggregated in the presence of negatively charged citrate coated AuNPs, the fluorescence of the equilibrium plateau was decreased, indicating inhibition leading to a reduction in the extent of aggregate formation

(Figure 2). This effect was dose dependent, ranging from no inhibition in the presence of 0.02 nM nanoparticles to 26 ± 13% inhibition in the presence of 0.1 nM nanoparticles. Further increase of the citrate coated nanoparticle concentration to 0.2 nM, however, failed to increase inhibitory capabilities.

The fluorescence of the equilibrium plateau was also decreased when $A\beta_{1-40}$ monomer was aggregated in the presence of PAH coated AuNPs, again indicating reduced aggregate formation (Figure 3). As for PAH coated AuNPs, this effect was dose dependent, ranging from 8 ± 3% inhibition in the presence of 0.025 nM nanoparticles to 42 ± 0% inhibition in the presence of 0.2 nM nanoparticles. Furthermore, these positively charged AuNPs were more effective inhibitors than citrate coated nanoparticles.

When $A\beta_{1-40}$ monomer was aggregated in the presence of negatively charged PAA coated AuNPs, any increase in fluorescence was abrogated, demonstrating complete inhibition of aggregate formation (Figure 4). Furthermore, this effect extended down to a concentration of 0.02 nM, a concentration that represents a substoichiometric ratio of 1:200 with $A\beta_{1-40}$ monomer.

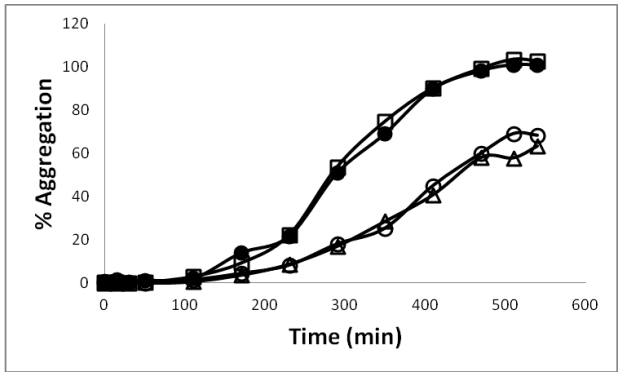

Figure 2. $A\beta_{1-40}$ monomer (40 μM) was incubated in 40 mM Tris-HCl alone (solid circle, control) or in the presence of 0.02 nM (open squares), 0.1 nM (open triangles), or 0.2 nM (open circles) citrate coated AuNPs. Aggregation was induced via vortexing at 25°C and monitored using ThT fluorescence. Results are representative of three independent experiments.

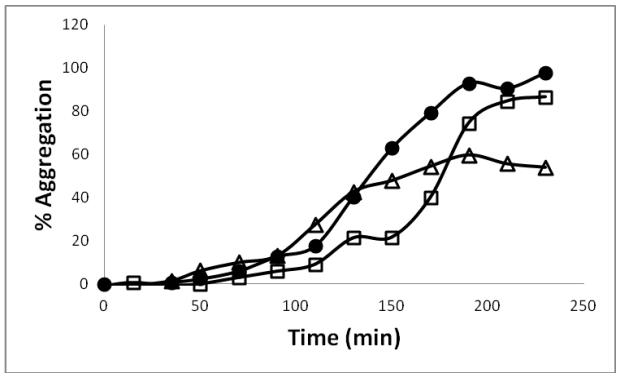

Figure 3. $A\beta_{1-40}$ monomer (40 μM) was incubated in 40 mM Tris-HCl alone (solid circles, control) or in the presence of 0.025 nM (open squares) or 0.2 nM (open triangles) PAH overcoated AuNPs. Aggregation was induced via vortexing at 25°C and monitored using ThT fluorescence. Results are representative of three independent experiments.

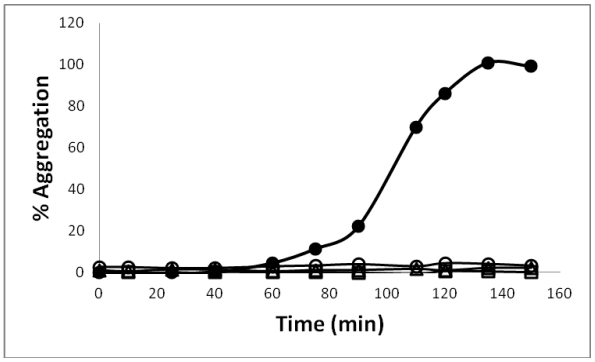

Figure 4. $A\beta_{1-40}$ monomer (40 μM) was incubated in 40 mM Tris-HCl alone (solid circles, control) or in the presence of 0.02 nM (open squares), 0.1 nM (open triangles), or 0.2 nM (open circles) PAA overcoated AuNPs. Aggregation was induced via vortexing at 25°C and monitored using ThT fluorescence. Results are representative of three independent experiments.

Table 1. Inhibition of $A\beta_{1-40}$ monomer aggregation by AuNPs with citrate, PAA, and PAH coatings.

AuNP coating	[AuNP]	% Inhibition[1]
Citrate	0.02 nM	0 ± 0%
	0.1 nM	26 ± 13%
	0.2 nM	30 ± 2%
PAH	0.025 nM	8 ± 3%
	0.2 nM	42 ± 0%
PAA	0.02 nM	100 ± 0%
	0.1 nM	100 ± 0%
	0.2 nM	100 ± 0%

[1]Monomer aggregation was performed in the presence of 18 nm AuNPs as in Figures 2-4. % Inhibition was calculated as the reduction in the fluorescence plateau at equilibrium, PR, using Eq. 1. Results represent the average of three independent experiments.

Thus, all three surface modified AuNPs were found to inhibit aggregation of $A\beta_{1-40}$ monomer in a dose dependent manner (Table 1). Furthermore, the extent of inhibition was influenced by surface overcoating, with negatively charged PAA coated nanoparticles exhibiting the most pronounced effects. These results are in agreement with the findings of Yoo et al. for CdTe nanoparticles [8] and Cabaleiro-Logo et al for copolymeric nanoparticles, where inhibition of Aβ aggregation was observed (9). These findings suggest that surface coated AuNPs may bind monomeric or oligomeric Aβ to reduce the concentration of the protein available for aggregation.

To explore the effect of nanoparticle size on inhibitory capabilities, PAA coated AuNPs with different diameters were investigated for their ability to inhibit $A\beta_{1-40}$ monomer aggregation. When the diameter of PAA coated AuNPs was reduced to 8 nm, their ability to inhibit $A\beta_{1-40}$ aggregation was

significantly reduced. Compared to the complete inhibition observed in the presence of 0.2 nM PAA coated AuNPs with a diameter of 18 nm, 8 nm PAA coated AuNPs were capable of reducing the fluorescence plateau by only 39 ± 19% (Figure 5, Table 2). This difference may result from the smaller surface area presented by smaller diameter AuNPs, reducing the ability of nanoparticles to sequester Aβ on their surface.

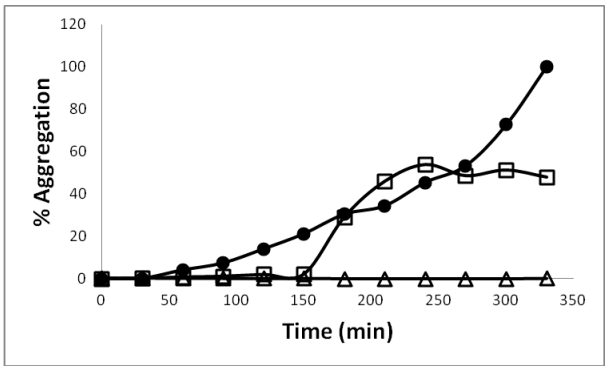

Figure 5. $A\beta_{1\text{-}40}$ monomer (40 μM) was incubated in 40 mM Tris-HCl alone (solid circles, control) or in the presence of 8 nm (open squares) or 18 nm (open triangles) PAA overcoated AuNPs present at a concentration of 0.2 nM. Aggregation was induced via vortexing at 25°C and monitored using ThT fluorescence. Results are representative of three independent experiments.

Table 2. Inhibition of $A\beta_{1\text{-}40}$ monomer aggregation by 8 nm and 18 nm PAA coated AuNPs.

AuNP diameter	[AuNP]	% Inhibition[1]
8 nm	0.2 nM	39 ± 19 %
18 nm	0.2 nM	100 ± 0 %

[1]Monomer aggregation was performed in the presence of PAA overcoated AuNPs as in Figure 5. % Inhibition was calculated as the reduction in the fluorescence plateau at equilibrium, PR, using Eq. 1. Results represent the average of three independent experiments.

Conclusions

The current study demonstrates that surface coated gold nanospheres are capable of inhibiting aggregation of Aβ, a process hypothesized to play a role in the progression of AD. Furthermore, both the surface coating and nanoparticle size play a role in the ability of AuNPs to intervene with the process of amyloid aggregation. These effects may stem from variations in the ability of AuNPs to interact with Aβ monomer or small oligomers and reduce the quantity of Aβ available for aggregation. Of particular significance, complete inhibition of 40 μM $A\beta_{1\text{-}40}$ monomer aggregation was observed in the presence of 0.02 nM PAA overcoated AuNPs. When considered relative to the low nanomolar concentrations of Aβ present *in vivo*, this 1:200 substoichiometric ratio represents an extremely low AuNP inhibitor concentration, which might be effectively delivered across the BBB. Together, these results suggest that AuNPs should be further explored as a therapeutic strategy for AD.

Acknowledgements

Funding for this project was provided by University of South Carolina Magellan Scholar Program and NSF-RUI grant #CHE-0701406.

References

1. Parihar, M. S., and Hemnani, T., *Journal of Clinical Neuroscience*, 2004, **11**, 456.
2. Minati, L., Edginton, T., Bruzzone, M. G., and Giaccone, G., *American Journal of Alzheimer's Disease & Other Dementias*, 2009, **24**, 95.
3. Goedert, M., and Spillantini, M. G., *Science*, 2006, **314**, 777.
4. LaFerla, F. M., Green, K. N., and Oddo, S., *Nature*, 2007, **8**, 499.
5. Reddy, P. H., and Beal, M. F., *Trends in Molecular Medicine*, 2007, **14**, 45.
6. Chithrani, B. D., Ghazani, A. A., and Chan, W. C. W., *Nano Letters*, 2006, **6**, 662.
7. Kanwar, J. R., Sun, X., Punj, V., Sriramoju, B., Mohan, R. R., Zhou, S. F., Chauhan, A., and Kanwar, R. K., *Nanomedicine*, 2011.
8. Yoo, S. I., Yang, M., Brender, J. R., Subramanian, V., Sun, K., Joo, N. E., Jeong, S. H., Ramamoorthy, A., and Kotov, N. A., *Angewandte Chemie International Edition*, 2011, **50**, 5110.
9. Cabaleiro-Lago, C., Quinlan-Pluck, F., Lynch, I., Lindman, S., Minogue, A. M., Thulin, E., Walsh, D. M., Dawson, K. A., and Linse, S., *Journal of the American Chemical Society*, 2008, **130**, 15437.
10. Connor, E. E., Mwamuka, J., Gole, A., Murphy, C. J., and Wyatt, M. D., *Small*, 2005, **1**, 325.
11. Murphy, C. J., Gole, A. M., Stone, J. W., Sisco, P. N., Alkilany, A. M., Goldsmith, E. C., and Baxter, S. C., *Accounts of Chemistry*, 2008.
12. Jana, N. R., Gearheart, L., Murphy, C.J., *Langmuir*, 2001, **17**, 6782.